Analysis of Climate Change Effects on Seawall Reliability

AUTHOR(S):

Mase, Hajime; Tamada, Takashi; Yasuda, Tomohiro; Karunarathna, Harshinie; Reeve, Dominic E.

CITATION:

Mase, Hajime ...[et al]. Analysis of Climate Change Effects on Seawall Reliability. Coastal Engineering Journal 2015, 57(03): 1550010.

ISSUE DATE:

2015-09

URL:

http://hdl.handle.net/2433/202838

World Scientific
www.worldscientific.com

JAPAN SOCIETY OF CIVIL ENGINEERS
COASTAL ENGINEERING COMMITTEE

Coastal Engineering Journal, Vol. 57, No. 3 (2015) 1550010 (18 pages)

DOI: 10.1142/S0578563415500102

Analysis of Climate Change Effects on Seawall Reliability

Hajime Mase*,§, Takashi Tamada†, Tomohiro Yasuda*,
Harshinie Karunarathna‡ and Dominic E. Reeve‡

*Disaster Prevention Research Institute,
Kyoto University, Gokasho, Uji, Kyoto 611-0011, Japan

†IDEA Consultants, Inc., 2-2-2 Hayabuchi,
Tsuduki, Yokohama, Kanagawa 224-0025, Japan

‡College of Engineering, Swansea University,
Singleton Park, Swansea SA2 8PP, UK

§mase.hajime.5c@kyoto-u.ac.jp

Received 26 January 2015
Accepted 25 May 2015
Published 13 August 2015

Crown heights of seawalls should be designed to suppress overtopping discharge to a permissible level. The permissible level is determined from viewpoints of the structure types of coastal seawalls and hinterland use. It is usually difficult to design the crown heights of seawalls, especially in the present time where climate change due to global warming is expected. This study analyzes climate change effects such as sea level rise (SLR) and increase of waves and surges on the failure probability of seawalls under various conditions of crown height, toe depth and slope by using a Level III reliability analysis. It was found that the difference of SLR trends (fast, medium or low) has less impact on overtopping rates than the differences in wave height change for a seawall at a target location.

Keywords: Climate change; wave overtopping; reliability analysis; failure probability.

1. Introduction

It is reported that the atmosphere and the oceans have warmed, the amounts of snow and ice have diminished and sea levels have risen as a result of global climate

change. IPCC [2014] projects more than a meter of sea level rise (SLR) at the end of this century in some parts of the world. With this, and with increasing stormy weather, coastal disasters are expected to be severe in future. We have experienced extreme tropical cyclones in recent years. In this context, research on coastal hazard evaluation and coastal defense structure design under climate change has become extremely important and timely [Mase *et al.*, 2013a; Mori *et al.*, 2013]. Under climate change conditions, researches on coastal defense structure design have become extremely important since many coastal structures in Japan were constructed in the latter half of the 1950s for given design parameters of wave heights and periods, storm surge heights and sea level. The structures themselves became obsolete and the external forces become larger.

The future wave climate projections have been conducted by a few researchers [e.g. Hemer *et al.*, 2006]. These studies have shown an increase in wave height due to increased wind speeds associated with mid-latitude storms in many regions of the mid-latitude oceans. Zhang *et al.* [2004] and Wang and Swail [2006] made statistical projections of global wave height from the empirical relationships between sea level pressure and significant wave height. In this context, climate change effects on safety performance of coastal structures should be considered in the design, maintenance and reconstruction of the coastal defense structures.

Coastal external forces that affect the failure of coastal structures are the sea levels, storm surges and high waves. By considering these parameters' change due to climate change, Mase *et al.* [2013a] analyzed a stability of composite breakwater covered with wave-dissipating blocks. In the present study, the failure probability of seawalls due to wave overtopping is analyzed. Crown heights of seawalls should be designed to suppress overtopping discharge into a permissible level. The permissible level is determined from viewpoints of the structure types of coastal seawalls and hinterland use. Since environmental coastal forces such as sea level, wave and storm surge have probabilistic nature, it is usually difficult to design the crown height, especially under the present time where climate change due to global warming is expected. This study analyzes climate change effects such as SLR and increase of wave and surge heights on failure probability of seawalls due to wave overtopping by using a Level III reliability analysis.

The random wave overtopping of seawalls can be estimated from design diagrams [e.g. Goda *et al.*, 1975; Tamada *et al.*, 2002] or by using various formulae [e.g. CEM by U.S. Army Corps of Engineers, 2002; TAW, 2002; EurOtop, 2007; Goda, 2009]. In most of the prediction models, input wave conditions are specified at offshore, at the toe of the foreshore slope, and at the toe of the structure itself. However, when a structure is built in very shallow water or on land, the wave height at its toe is not easy to define. Mase *et al.* [2013b] proposed the prediction model linking wave runup and overtopping on seawalls built on land and in very shallow water. This model is used in the present study for evaluating the failure probability of seawalls.

Section 2 in this paper gives a description of reliability analysis and failure functions related to wave overtopping. In Sec. 3, target analyzed conditions of topography, seawall, wave height, period, sea level and so on are described. Section 4 shows the failure probabilities of seawalls from the present to future, and Sec. 5 describes discussion and conclusions.

2. Reliability Analysis and Failure Functions Related to Wave Overtopping

2.1. *Reliability analysis*

Reliability analysis quantifies the probability of occurrence of a particular failure mode represented by the failure function $Z = f(X_1, \ldots, X_N)$ where X_i are the random variables with a probability density function involved in the concerned problem. The failure function, Z, is generally a nonlinear function of the random variables. The probability of failure, P_f, is then written as follows:

$$P_f = P(Z \leq 0) = \iint_{Z \leq 0} \cdots \int f(X_1, \ldots, X_N) dX_1 \cdots dX_N. \tag{1}$$

The above equation is the mathematical basis for probabilistic analysis. The above integrations cannot be performed analytically and have to be approximated in some way. They are classified on the basis of the types of calculations performed and of the approximations made [see, e.g. Thoft-Christensen and Baker, 1982; Melchers, 1999; Reeve, 2009]. In general, three common levels are defined, in order of decreasing accuracy, as follows:

(1) Level III: Full distribution approach
    This method provides an exact probabilistic analysis for whole variables by using full joint probability density functions including the correlations among the variables.
(2) Level II: Semi-probabilistic approach
    Approximation methods that the correlated and non-normal variables are transformed into uncorrelated and normal variables are employed. Reliability indices are used as measures of the structure safety. Nonlinear failure functions are approximated using a tangent hyper plane at some point. If linearization is performed about the expected mean values of the variables, the method is known as the first-order mean value approach, FOMVA. If the failure function is linearized about the point in the failure surface having the highest joint probability density, the method is called a first-order reliability method, FORM.
(3) Level I: Limit state approach
    This approach is based on the use of characteristic values and partial load and resistance factors. The factors represent the ratio of load at failure to permissible

working load. This allows a desired margin between the characteristic values of resistance and working load. Level I approach does not describe the reliability (or the failure probability) of the design.

In the present study, the Level III approach is used to estimate the failure probability of seawall due to wave overtopping with a Monte Carlo simulation technique.

2.2. *Failure functions*

Permissible wave overtopping discharges are determined for functional and structural safety, and structure types of seawalls and hinterland use, although there are several pathways to final collapse of seawalls and coastal flooding. For seawall overtopping, the failure means that the specified permissible overtopping rate is exceeded. Acceptable probabilities of failure per year are often between 0.01% and 1% but can be higher when considering functional safety alone. These acceptable probabilities are better determined by comparing them with other kinds of risks and the acceptable probability of failure depends on the consequences of failure.

Structural damages of seawalls are, for example, parapet collapse, upper surface fracturing, slope armoring breakage, toe scouring and rear ground scouring. All failure modes must be identified and examined as the possible risks of seawall damage. Negligence of an important failure mode will bias the estimation of the safety of the structure. Since, however, it is not generally known how to quantify such failure modes (failure functions), the present study takes up two failure modes as shown in Fig. 1. Figure 1(a) shows the failure mode where the overtopping discharge exceeds a permissible level. Figure 1(b) is the failure mode where overtopping waves break the upper concrete plate where a void is assumed to be present under the concrete plate.

The failure function corresponding to Fig. 1(a) is written as

$$Z = q_a - q, \tag{2}$$

where q_a is the permissible overtopping discharge ($m^3/s/m$), and q the value estimated from the prediction formula of Mase *et al.* [2013a], which is an extended version of Hedges and Reis [2004], as

$$\frac{q}{\sqrt{gH_0^3}} = \begin{cases} 0.018\left(\dfrac{R_{\max}}{H_0}\right)^{\frac{3}{2}}\left\{1-\left(\dfrac{R_c}{H_0}\right)\Big/\left(\dfrac{R_{\max}}{H_0}\right)\right\}^{6.240}, & \text{for } 0 \le R_c \le R_{\max}, \\ 0, & \text{for } R_{\max} < R_c, \end{cases} \tag{3}$$

$$R_{\max} = 1.54H_0\{2.99 - 2.73\exp(-0.57\tan\beta/\sqrt{H_0/L_0})\}, \tag{4}$$

when using $(R_{\max})_{99\%,100}$ (the value not exceeded in 99% of the cases assuming a Rayleigh distribution) where $\tan\beta$ is the imaginary slope and H_0 offshore wave height.

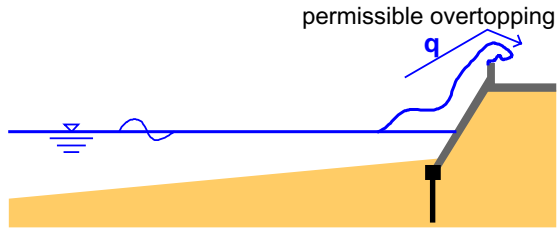

(a)

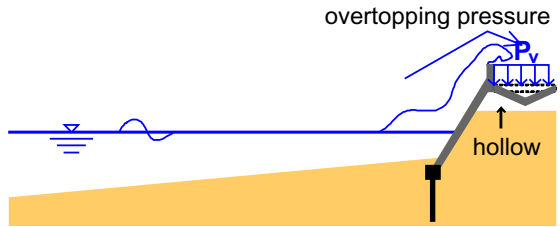

(b)

Fig. 1. Failure of seawall by excess overtopping and pressure.

The failure function corresponding to Fig. 1(b) is given by

$$Z = \sigma_y - \frac{M(P_v, B)}{Z_d}, \tag{5}$$

where σ_y is the tensile yield strength $(\mathrm{N/mm^2})$, $M(P_v, B)$ is the bending moment $(\mathrm{kN \cdot m})$ determined from overtopping wave pressure and length of the hole, Z_d the section modulus $(\mathrm{m^3})$. For the value of σ_y, 0.67 N/m is employed according to "Specifications for Highway Bridges" by the Japan Road Association [2005]. The value of Z_d is set to $0.0417\ \mathrm{m^3}$ under the conditions of unit width 1.0 m and concrete thickness 0.5 m.

The wave pressure of overtopping wave was formulated as follows. Imai *et al.* [2010] investigated wave pressures of overtopping waves on road of seawall in which the relations between offshore wave heights, overtopping discharges and wave pressures are shown. From the figures, the relation between the overtopping discharges and wave pressures was re-arranged as shown in Fig. 2. Although the dimensions of vertical and horizontal axes are different, the line represents the upper trend of experimental results. The present study employs the following equation:

$$p_v = 10{,}830q, \tag{6}$$

where the dimension of p_v is $\mathrm{kN/m^2}$.

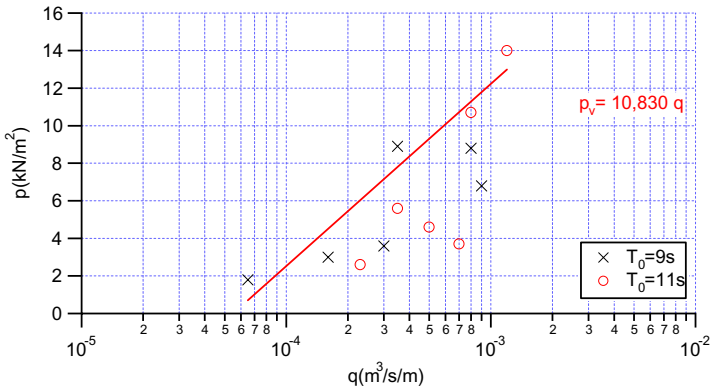

Fig. 2. Relation between overtopping discharge and wave pressure.

3. Target Conditions

3.1. *Conditions of seawall*

For evaluation of climate change effects on seawall failure, the target seawall is set considering a real seawall installed on the coast of Kochi Prefecture, Japan, facing the Pacific Ocean which is exposed to extreme waves [Shimura *et al.*, 2011]. Figure 3 shows the seawall at the site.

From the National Association of Sea Coast [2008], the configuration of a seawall is that the crown height is T.P. (Tokyo Peil) +10 m, the front slope is 1:0.5 built on a sandy beach of 1/20 slope. This configuration is taken as a basic one. In addition, in order to know how much the failure probabilities change depending on the seawall

Fig. 3. Photo of seawall at a coast of Kochi, Japan.

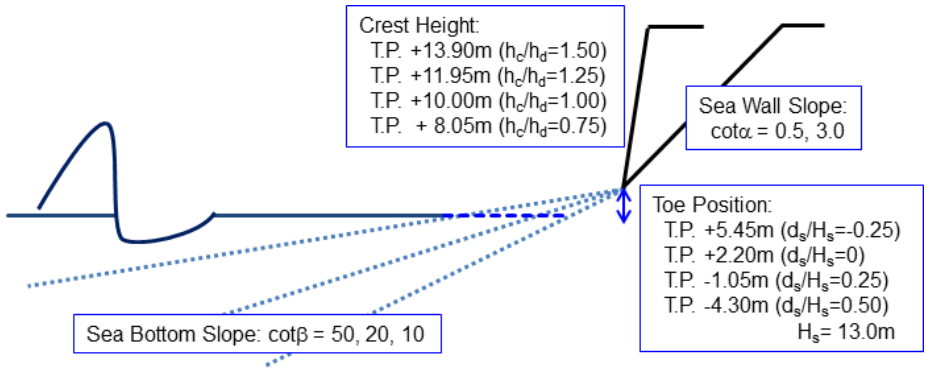

Fig. 4. Target analyzed conditions of seawall and foreshore beach.

conditions, the following values of the key variables are changed: the crown heights of T.P. +13.90 m, 11.95 m, 10.00 m, 8.05 m; the seawall slope, $\cot\alpha$, as 0.5 and 3.0; the toe depth, d_s, as T.P. +5.45 m, 2.20 m, −1.05 m, −4.30 m and foreshore slope, $\cot\beta$, 50, 20 and 10. Figure 4 summarizes the calculation conditions of seawall size and beach slope.

3.2. *Setting of external forces — Sea conditions*

The SLR is a component of climate change and is important for human activity near the coastal zone. Global sea level increased by 1.8 mm/year from 1961–2003 and 3.1 mm/year from 1993–2003 [IPCC, 2007], and IPCC AR4 indicates that the projected minimum and maximum SLR at the end of 21st century are 0.18–0.59 m depending on different scenarios and general circulation model output, and the corresponding figures from IPCC AR5 are 0.26–0.98 m. Mori *et al.* [2013] summarized the SLR by arranging all available CMIP3 models for A2, A1B and B2 scenario around Japan. Figure 5 shows the SLR trend in Japan region obtained from CMIP3 for the A1B scenario. The mean SLR trend around Japan is slightly different from the global trend. The mean (GCM model ensemble) trend is denoted as SL-M, the large one with one standard deviation added shown by SL-L and the small one with one standard deviation subtracted as SL-S. These three SLR trend were adopted in the analysis.

The future wave heights with 50 years return period, estimated from wave simulations from 2075 to 2100 will increase by 1.23 times compared to the present offshore wave heights around Kochi Prefecture [Shimura *et al.*, 2011]. According to the projection, the present design wave height of 13.0 m is multiplied by 1.23 in 87.5 years time as shown in Fig. 6 together with two other lines representing plus and minus one standard deviation to the mean trend mean trend [Shimura *et al.*, 2011]. The highest trend line is denoted as WA-L, the mean trend as WA-M and the lower trend as WA-S. The linear increase in wave height was assumed since the near future wave simulation was not carried out.

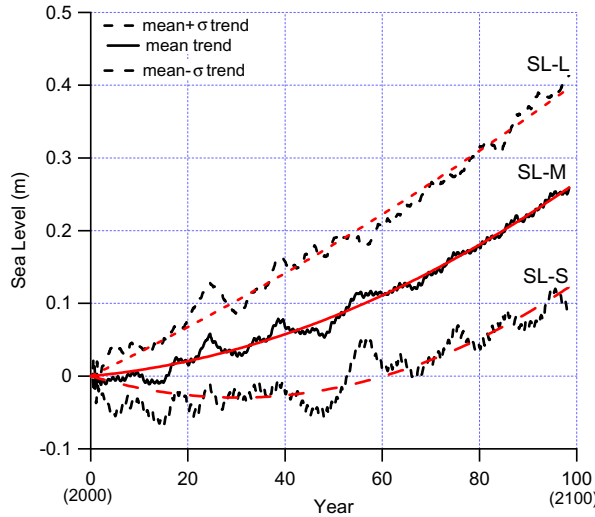

Fig. 5. Trend of SLR.

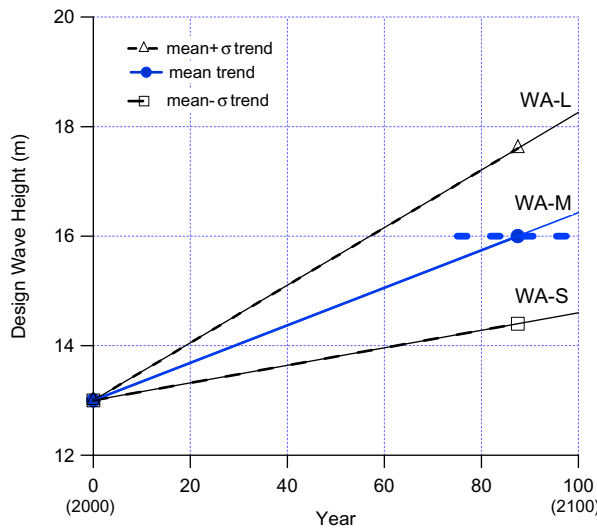

Fig. 6. Trend of wave height.

The Weibull distribution is employed as the offshore wave height distribution of which shape parameter κ is 1.4 and scale parameter is given by

$$A = 0.0526t + 13; \quad \text{for WA-L} \tag{7}$$

$$A = 0.0343t + 13; \quad \text{for WA-M} \tag{8}$$

$$A = 0.0160t + 13; \quad \text{for WA-S} \tag{9}$$

so that the 50 years return wave heights from the Weibull distribution match the trend lines in Fig. 6. The 100 years return wave height is used as the upper limit to prevent abnormally large wave height.

Reeve [1998] used a functional relationship, of the form $T = aH^b$, to link wave height and period explicitly in a Level II analysis of wave overtopping of sea defenses. The rationale behind this is a putative scaling law such that waves retain a constant steepness as their severity increases. If these were exactly the case then $b = 0.5$ is the constant for linear waves. Goda [2003] proposed an averaged relationship between the significant wave height and period as follows:

$$T_s \approx 3.3H_s^{0.63}. \tag{10}$$

Since the design wave at Kochi coast is $T_s = 15.5\,\mathrm{s}$ for a wave height $H_s = 13.0\,\mathrm{m}$, the above equation was modified to

$$T_s \approx 3.08H_s^{0.63}. \tag{11}$$

The distribution of wave periods is taken as a normal distribution with a mean of T_s from Eq. (11) and the standard deviation of $0.05T_s$ for a given H_s from the Weibull distribution.

For the distribution of tides, a triangle distribution with the maximum level of T.P. $+0.72\,\mathrm{m}$, minimum level of T.P. $-1.07\,\mathrm{m}$ and mode of T.P. $+0.25\,\mathrm{m}$ was employed from the observation at Kochi Port.

The surge height, η, is related to the wave height H_s; the distribution of η is given by a normal distribution with a mean value of $\mu = 0.1H_s$ and standard deviation of $\sigma = 0.1\mu$. The upper and lower limits are set as $(\mu + 2\sigma)$ and $(\mu - 2\sigma)$. Although the relation between surge and wave heights are not well known, the present method followed Goda and Takagi [2000] and Suh *et al.* [2012] where the surge height is assumed to be 10% of the deepwater significant wave height. In addition, the assumed surge heights are distributed using normal distribution in this study.

3.3. *Calculation of reliability*

Probabilities of failure were estimated by sampling values of the key variables according to the distributions specified above and performing Monte Carlo simulations of 10,000 realizations in order to estimate the probabilities of failure (the rate that the failure function becomes zero and negative) for each specific case.

4. Computed Failure Probabilities

4.1. *Failure of seawall by large overtopping*

Figure 7 shows a change of failure probability a year interval from the present into the future for the seawall with the current design crown height ($h_c/h_d = 1.0$) built on land ($d_s/H_s = -0.25$) of foreshore slope ($\cot\beta = 20$); figure (a) is the case of

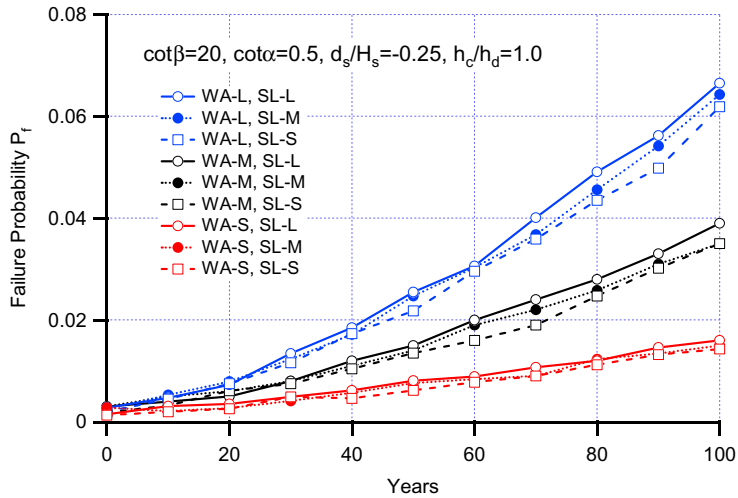

(a)

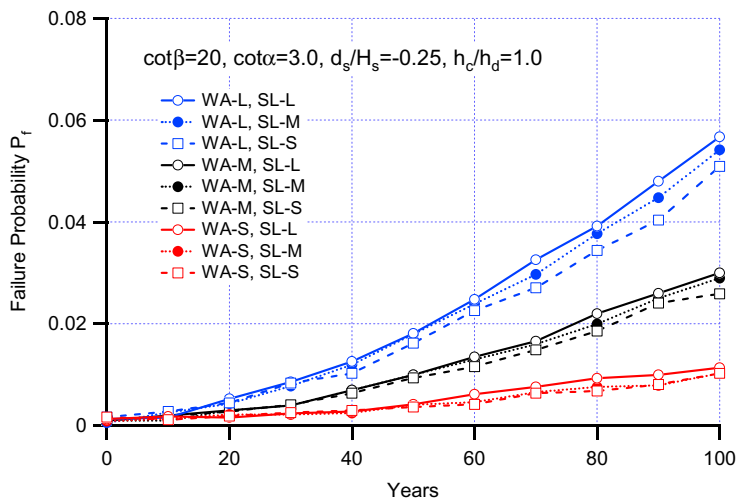

(b)

Fig. 7. Failure probability trend of seawall with the present crown height built on land over 1/20 foreshore beach: (a) steep slope seawall and (b) gentle slope seawall.

steep slope seawall ($\cot\alpha = 0.5$) and figure (b) gentle slope seawall ($\cot\alpha = 3.0$). It is seen from these figures that the effect of different SLR changes of SL-L, SL-M and SL-S is small compared to the effect of difference in wave height change as WA-L, WA-M and WA-S, although, of course, the larger the SLR trend is, the larger the failure probability is. The SLR is often said to be a threat to coastal disasters. However, the increase in wave heights induces much severe problems for stability of coastal structures.

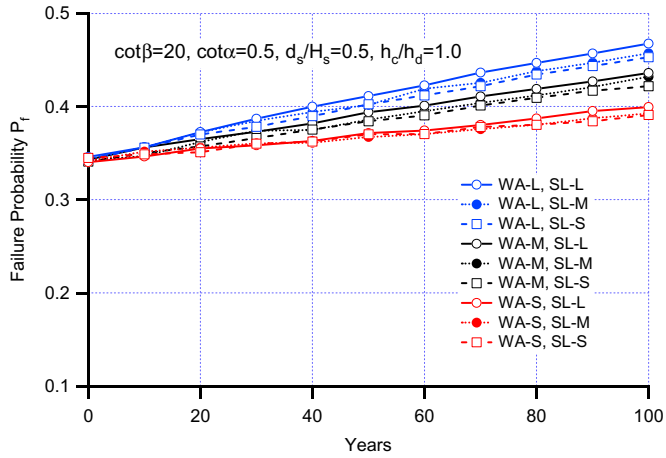

(a)

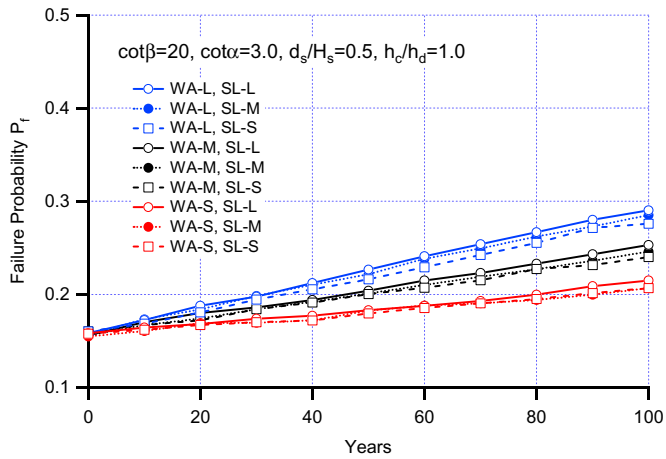

(b)

Fig. 8. Failure probability trend of seawall build in sea over 1/20 foreshore beach: (a) steep slope seawall and (b) gentle slope seawall.

When the seawall is installed in sea ($d_s/H_s = 0.5$), the failure probabilities are one order larger than those built on land as seen in Fig. 8. These results also show that the effect of different sea level changes is small compared to the effect of changes in wave height, since the difference in range is at most 0.3 m but difference in wave height about 4 m. The difference in the failure probabilities due to seawall slope is pronounced compared to Fig. 7 in the case seawalls set in sea.

Estimations of failure probabilities were carried out for all conditions of seawall and external forces by changing the crown height, toe depth, seawall slope and foreshore slope. Figure 9 shows the change of failure probability for the steep sloped seawall with the present crown height from the present to near future after 20 years

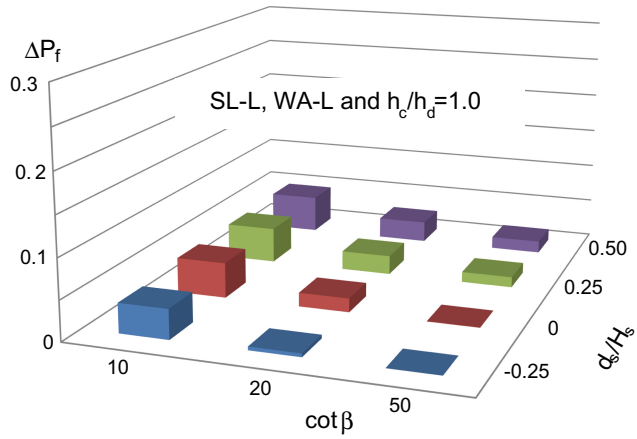

Fig. 9. Change of failure probability for steep slope seawall with the present crown height 20 years later under the conditions of large SLR trend and large wave height change trend.

under the conditions of the large SLR trend SL-L and large wave height trend WA-L. It is generally seen that the steeper the foreshore slope becomes, the larger the failure probability increases. When the foreshore slope is 1/10, the increase of the failure probability due to the difference of toe depth d_s/H_s is not remarkable; however for gentler foreshore slope such as $\cot\beta = 20$ and 50, it becomes larger according to the toe depth d_s/H_s.

Figure 10 shows the failure probability against the normalized crown height of steep seawall (plotted by black symbols and lines) and gentle seawall (red symbols and lines), installed at the shore line $d_s/H_s = 0$ on 1/20 foreshore beach, for present, 50 and 100 years later. Similarly to Fig. 10, Fig. 11 displays the failure probability against the normalized toe depth of steep seawall (black symbols and lines) and gentle seawall (red symbols and lines), with the present crown height $h_c/h_d = 1.0$,

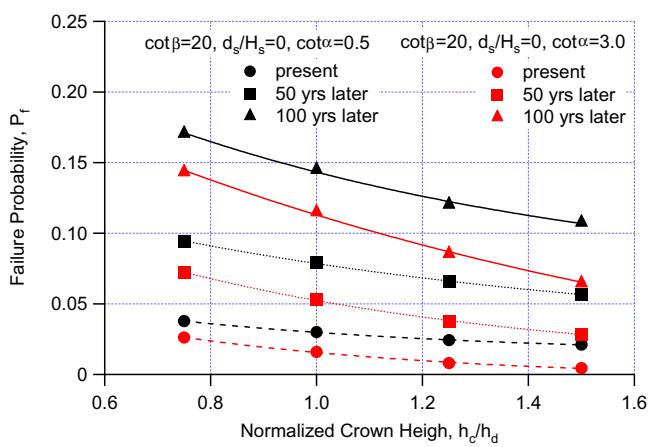

Fig. 10. Failure probability against the normalized crown height for present, 50, 100 years later.

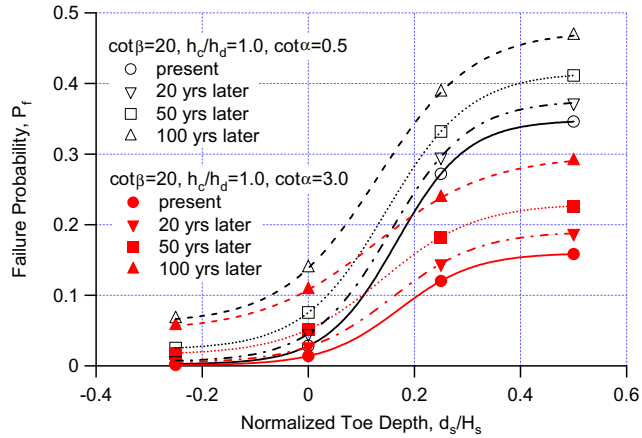

Fig. 11. Failure probability against the normalized toe depth for present, 20, 50, 100 years later.

for present, 20, 50 and 100 years hence. It is seen from these figures that the failure probabilities for each period do not change against the crown height so much; however, those against the toe depth change remarkably. When the seawalls are installed on land (when $d_s/H_s < 0$), the change of the failure probabilities from the present to future is small as shown in Fig. 11.

4.2. *Failure of seawall by overtopping pressure*

As a failure mode comes from the upper surface fracturing by overtopping, Fig. 12 shows the time history of failure probability of steep seawall with the present design

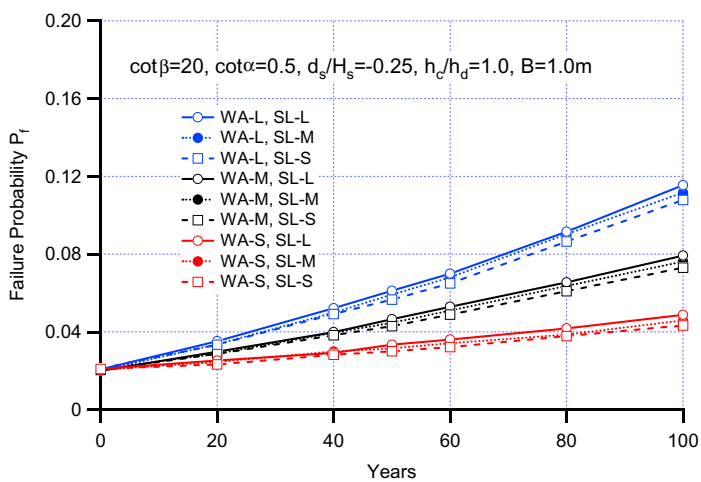

(a)

Fig. 12. Failure probability trend of steep slope seawall with the present crown height over 1/20 foreshore beach: (a) seawall on land and (b) seawall in sea.

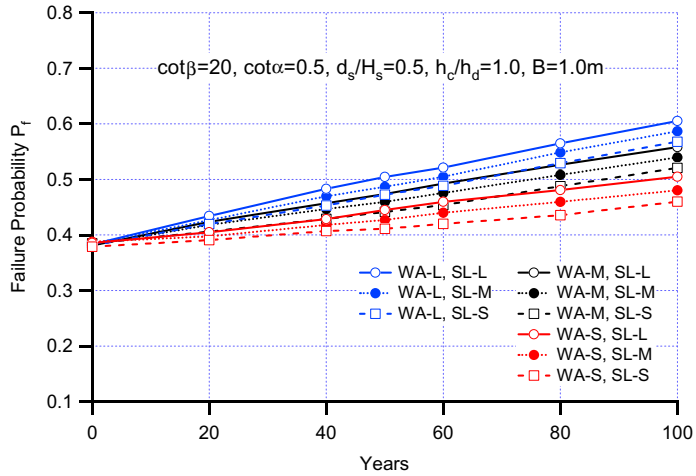

(b)

Fig. 12. (*Continued*)

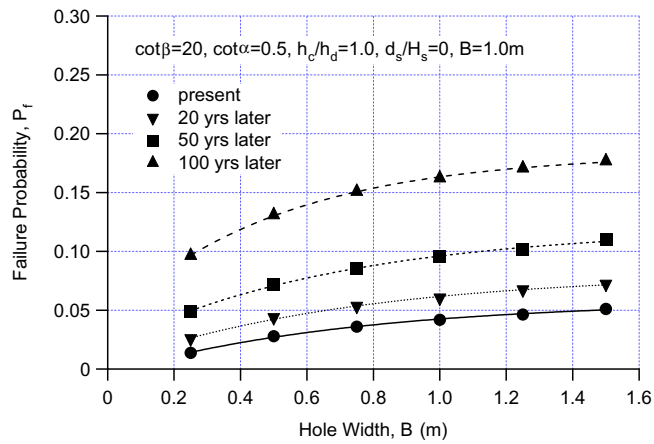

Fig. 13. Failure probability against the hole width for present, 20, 50, 100 years later.

crown height installed on 1/20 foreshore beach under the condition having a 1.0 m hole; figure (a) is for the seawall built on land, and figure (b) for the seawall built in sea. As in Figs. 7 and 8, the effect of different SLR change trends is small compared to the effect of changes in wave height, and the failure probability becomes large when the toe depth is large. Figure 13 shows the change of the failure probability of steep seawall, with the present design crown height on 1/20 foreshore slope beach, against the hole width. The failure probability becomes constant for a hole width due to the occurrence probability of wave overtopping.

Figures 14 and 15 show the failure probabilities against the normalized crown height and normalized toe depth, respectively, of steep seawall (in black) and gentle

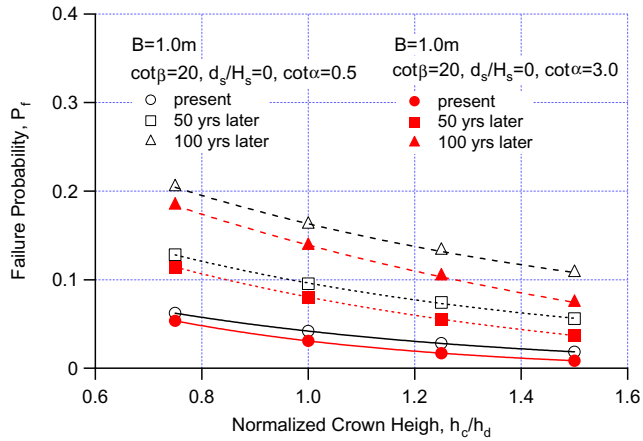

Fig. 14. (Color online) Failure probability against the normalized crown height hole width for present, 20, 50, 100 years later.

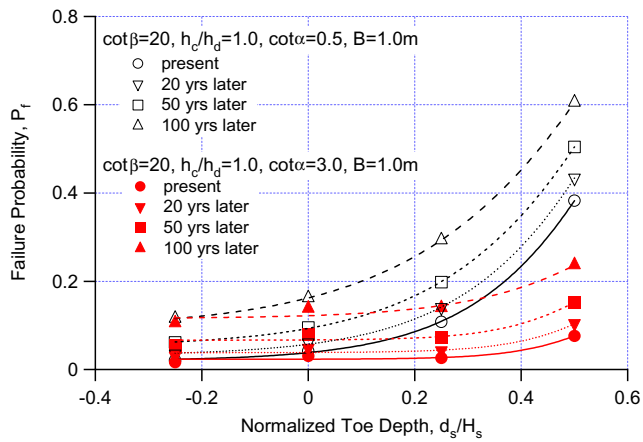

Fig. 15. (Color online) Failure probability against the normalized toe depth for present, 20, 50, 100 years later.

seawall (in red) for present time, 20, 50 and 100 years later where foreshore slope is 1/20 in the case of 1.0 m hole width. The change rate of failure probability of seawall with gentle slope seawall is smaller even if the toe depth becomes larger compared to Fig. 11.

5. Discussion and Conclusions

There are several pathways that can lead to the failure of seawalls as shown in Fig. 16 where the probability of each path occurring is shown as p_1–p_4. Using a permissible wave overtopping does not reflect the actual process of damage progression but employs a representative value of overtopping discharge. That is, it provides

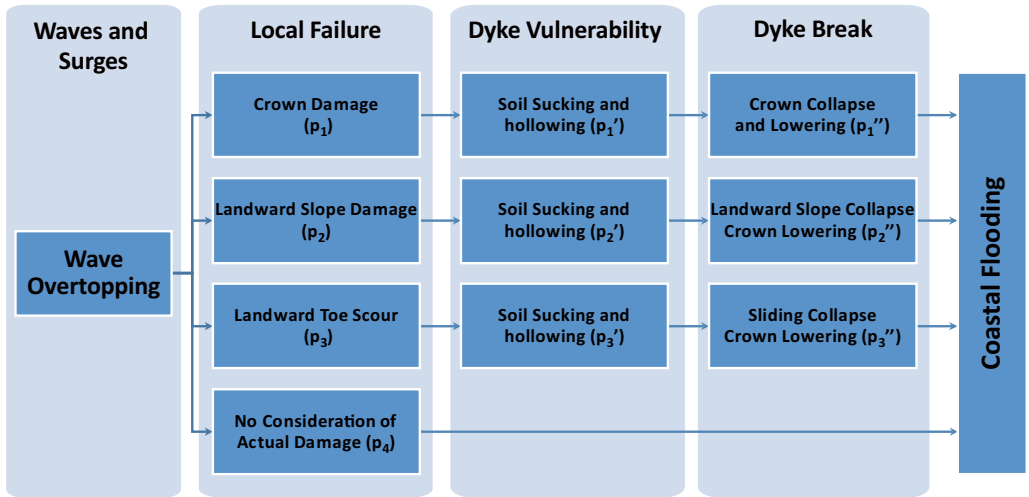

Fig. 16. Failure pathways for seawalls.

a snapshot of the risk at a particular time, assuming the integrity of the seawall is unchanged. Including time varying seawall integrity adds significant complexity to the problem [Hedges and Reeve, 2011]. The present study estimated the failure probability of p_4 in Fig. 16. The analysis considering the upper surface fracturing corresponds to the first pathway from crown damage to crown collapse and lowering in which the failure probability is given by multiplication of $p_1 p_1' p_1''$. A final failure probability may be represented by

$$P_f = \{(p_1 \times p_1' \times p_1''), \text{or } (p_2 \times p_2' \times p_2''), \text{or } (p_3 \times p_3' \times p_3''), \text{or } p_4\}. \tag{12}$$

The present study only estimated the failure probability of p_1, but not p_1' and p_1'' since these are not clear. The failure probabilities due to the landward slope damage and landward toe scour require additional variables and were not calculated in this study due to their complexity.

The present study analyzed the effects of climate change on the failure probabilities of seawalls where sea level, waves and surges are changed toward future, by using a Level III reliability analysis method. The target conditions were setup by considering the prevailing conditions at a seawall installed in the Kochi Prefecture, Japan. It was found that different SLR trends represented by the mean (GCM model ensemble) trend, the large one as the mean trend plus the standard deviation and the small one as the mean trend minus standard deviation did not have a large impact on the failure probabilities of seawalls; however, the effect of differences in wave height trend is more remarkable.

One of the adaptation methods of upgrading seawalls for climate change (global warming) is to modify the structure so as to keep the present safety level. For example, referring to Figs. 10 and 11, the failure probability (or conversely, the

safety level) in future can be estimated for a given condition of crown height, toe depth and seawall slope by employing the reliability calculations; from which, the upgrading seawall crown height can be obtained so as to keep the present safety level.

Acknowledgments

A part of this study was supported by SOUSEI program and KAKENHI Grand-in-Aid by the Ministry of Education, Culture, Sports, Science, and Technology (MEXT), Japan. The authors express their particular gratitude to Associate Professor Nobuhito Mori for his valuable opinions and to Master Course Student Mr. Takanobu Aimatsu for his arrangement of data.

References

EurOtop [2007] *Wave Overtopping of Sea Defences and Related Structures*: *Assessment Manual*, eds. Pullen, T., Allsop, N. W. H., Bruce, T., Kortenhaus, A., Schuttrumpf, H. & van der Meer, J. W., Available at http://www.overtopping-manual.com/manual.html.

Goda, Y. [2003] "Revisiting Wilson's formulas for simplified wind-wave prediction," *J. Waterway Port Coastal Ocean Eng. ASCE* **129**(2), 93–95.

Goda, Y. [2009] "Derivation of unified wave overtopping formulas for seawalls with smooth, impermeable surfaces based on selected CLASH datasets," *Coastal Eng.* **56**, 385–399.

Goda, Y. & Takagi, H. [2000] "A reliability design method of caisson breakwaters with optimal wave-heights," *Coastal Eng. J.* **42**(4), 357–387.

Goda, Y., Kishira, Y. & Kamiyama, Y. [1975] "Laboratory investigation on the overtopping rate of seawalls by irregular waves," *Rept. Port Harbour Res. Inst.* **14**(4), 3–44 (in Japanese).

Hedges, T. S. & Reis, M. T. [2004] "Accounting for random wave run-up in overtopping predictions," *Proc. Inst. Civil Engineers, Maritime Eng. J.* **157**, 113–122.

Hedges, T. S. & Reeve, D. E. [2011] "Discussion of time-dependent risk assessment of combined overtopping and structural failure for reinforced concrete coastal structures," by Li. C. Q. & Zhao, J. M., *J. Waterway Port Coastal and Ocean Eng.*, *ASCE* **137**, 210–211.

Hemer, M., Church, J., Swail, V. & Wang, X. [2006] "Coordinated global wave climate projections," *Atmosphere-Ocean Interact.* **2**, 185–218.

Imai, K., Kimura, K., Shimizu, T. & Kamikubo, K. [2010] "Hydraulic model test on wave overtopping for a coastal road," Research Report Hokkaido Branch of JSCE, **B-47**, 2 (in Japanese).

IPCC [2007] IPCC Fourth Assessment Report (AR4), Available at http://www.ipcc.ch/.

IPCC [2014] IPCC Fifth Assessment Report (AR5), Available at http://www.ipcc.ch/index.htm.

Japan Road Association [2005] *Specifications for Highway Bridges*, 540p. ISBN: 978-4-88950-709-6 (in Japanese).

Mase, H., Tsujio, D., Yasuda, T. & Mori, N. [2013a] "Stability analysis of composite breakwater with wave-dissipating blocks considering increase in sea levels, surges and waves due to climate change," *Ocean Eng.* **71**, 58–65, doi: 10.1016/j.oceaneng.2012.12.037.

Mase, H., Tamada, T., Yasuda, T., Hedges, T. S. & Reis, M. T. [2013b] "Wave runup and overtopping at seawalls built on land and in very shallow water," *J. Waterway Port Coastal Ocean Eng. ASCE* **139**(5), 346–357, doi: 10.1061/(ASCE)WW.1943-5460.0000199.

Melchers, R. E. [1999] *Structural Reliability Analysis and Prediction*, 2nd edn. (John Wiley & Sons, Chichester), 437p.

Mori, N., Shimura, T., Yasuda, T. & Mase, H. [2013] "Multi-model climate projections of ocean surface variables under different climate scenarios — Future change of waves, sea level and wind," *Ocean Eng.* **71**, 122–129, doi: 10.1016/j.oceaneng.2013.02.016.

National Association of Sea Coast [2008] Progress of sea coast 50 years, Coastal Division of River Department, Ministry of Land, Infrastructure, Transport and Tourism, 930p. (in Japanese).

Reeve, D. E. [1998] "On coastal flood risk," *J. Waterway Port Coastal Ocean Eng. ASCE* **124**(5), 219–228.

Reeve, D. E. [2009] *Risk and Reliability: Coastal and Hydraulic Engineering* (SPON Press, London), 304p.

Shimura, T., Mori, N., Nakajyo, S., Yasuda, T. & Mase, H. [2011] "Extreme wave climate change projection at the end of 21st century," *Proc. of 6th Int. Conf. on Asian and Pacific Coasts (APAC 2011)*, 341–348.

Suh, K.-D., Seung-Woo Kim, S.-W., Mori, N. & Mase, H. [2012] "Effect of climate change on performance-based design of caisson breakwaters," *J. Waterway Port Coastal and Ocean Eng. ASCE* **138**(3), 215–225.

TAW [2002] "Technical report wave run-up and wave overtopping at dikes," ed. Van der Meer, J. W. (Technical Advisory Committee on Flood Defense, The Netherlands), 50p.

Tamada, T., Inoue, M & Tezuka, T. [2002] Experimental Studies on diagrams for the estimation of wave overtopping rate on gentle slope-type seawalls and these reduction effects on wave overtopping," *Proc. Coastal Eng., JSCE* **49**, 641–645 (in Japanese).

Thoft-Christensen, P. & Baker, M. J. [1982] *Structural Reliability Theory and Its Applications* (Springer, Berlin).

U.S. Army Corps of Engineers [2002] Coastal Engineering Manual (CEM), Engineer Manual 1110-2-1100, Washington, D.C.

Wang, X. & Swail, V. [2006] "Historical and possible future changes of wave-heights in Northern Hemisphere oceans," *Atmosphere-Ocean Interact.* **2**, 185–218.

Zhang, K., Douglas, B. & Leatherman, S. [2004] "Global warming and coastal erosion," *Climatic Change* **64**(1), 41–58.